American Mineralogist, Volume 74, pages 1207–1214, 1989

Mineralogical studies of the nitrate deposits of Chile: VI. Hectorfloresite, $Na_9(IO_3)(SO_4)_4$, a new saline mineral

George E. Ericksen, Howard T. Evans, Jr., Mary E. Mrose, James J. McGee, John W. Marinenko, Judith A. Konnert
U.S. Geological Survey, Reston, Virginia 22092, U.S.A.

Abstract

The new mineral hectorfloresite, known to occur in only one locality in the nitrate fields of northern Chile, consists of tiny prismatic crystals, generally less than 1 mm long and 0.2 mm in diameter, in cavities in dense nitrate ore consisting of saline-cemented silt, sand, and small rock fragments. The cavities also contain euhedral crystals of halite, darapskite, and glauberite. Hectorfloresite is named for Hector Flores W. (1906–1984), a pioneer Chilean geologist.

Hectorfloresite is monoclinic and occurs as pseudohexagonal prismatic crystals consisting of multiple prismatic twins. The space group is $P2_1/a$, with a = 18.775(4) Å, b = 6.9356(7) Å, c = 14.239(2) Å, β = 108.91(2)°, and Z = 4[$Na_9(IO_3)(SO_4)_4$]. X-ray powder patterns of natural hectorfloresite show the following strong lines (d_{meas}, I/I_0, hkl): 3.880(100)($\bar{4}11$), 2.700(80)($\bar{6}04$), 2.788(30)(222), 1.9420(20)($\bar{8}22$), 4.69(15)($\bar{4}01$), 6.17(10)(011), 1.6800(10)(632), 1.5607(10)(606), and 1.5533(10)($\bar{6}09$). Crystal forms are $a\{100\}$, $c\{001\}$, and $q\{212\}$. The new mineral has a hardness of about 2, lacks cleavage, and shows a conchoidal fracture. The measured specific gravity of synthetic hectorfloresite is 2.80(3) and the calculated density is 2.90 g/cm³. Hectorfloresite is biaxial negative with α = 1.493(2), β = 1.521(2), and γ = 1.523(2); $2V_X$ = 26(2)°. The new mineral is one of two double salts in the system $NaIO_3$-Na_2SO_4-H_2O. Microprobe analyses of crystals of natural hectorfloresite show the average composition to be 34.5% Na_2O, 23.2% I_2O_5, and 42.3% SO_3. Chemical analyses of synthetic hectorfloresite show essentially the same composition. The formula based on these analyses is $Na_9(IO_3)(SO_4)_4$. This composition was confirmed by crystal-structure analysis of natural hectorfloresite.

Introduction

The new mineral hectorfloresite occurs as tiny, white, prismatic crystals in slitlike cavities in nitrate ore at the Alianza mine (Rajo #13) of Oficina Victoria, Province of Tarapacá, Chile. This mine was active in 1962 when the specimens containing hectorfloresite were collected, and the ore, which averaged about 8% $NaNO_3$, was treated at the Oficina Victoria beneficiation plant. This operation closed in 1979, and the plant and townsite at Oficina Victoria were subsequently dismantled. Nitrate ore in Rajo #13 was mined out, and it is not now possible to precisely locate the specimen site.

The hectorfloresite-bearing cavities are subhorizontal, lenticular desiccation fissures, as much as 30 cm in diameter and several centimeters wide, that occur in dense, brown nitrate ore consisting of sand, silt, and small rock fragments firmly cemented by saline minerals. The principal saline minerals in nitrate ore of this type are halite [NaCl], nitratine [$NaNO_3$] (according to Fleischer, 1987, this name takes precedence over the earlier names, soda niter and nitratite, previously used in this series of reports on mineralogy of the Chilean nitrate deposits), darapskite [$Na_3(NO_3)(SO_4)\cdot H_2O$], blödite [$Na_2Mg(SO_4)_2\cdot 4H_2O$], glauberite [$Na_2Ca(SO_4)_2$], and other, generally less abundant sulfate minerals. The cavities are lined with euhedral crystals of halite, darapskite, and glauberite, in addition to hectorfloresite. Single crystals and clusters of crystals (Fig. 1) of hectorfloresite are intergrown with small (<2-mm diameter) glauberite crystals and occur as sparse overgrowths on this mineral and halite. Large (as much as 2 cm in diameter) darapskite plates were apparently the last mineral to form in the cavities because they cover both glauberite and halite but do not have hectorfloresite overgrowths. Furthermore, SEM photographs show clusters of parallel, microscopic darapskite plates on a few hectorfloresite crystals.

The specimens were collected because they contained the large plates of darapskite, and the tiny crystals of hectorfloresite were not discovered until subsequent laboratory study. X-ray powder-diffraction films of these crystals indicated a mineral that had not previously been described, and microchemical tests showed the presence of sulfate, but otherwise were inconclusive. Inasmuch as the total amount of material available (a few milligrams) was not sufficient for a chemical analysis, the mineral was set aside for possible future study.

In 1986, hectorfloresite crystals were examined by SEM

0003–004X/89/0910–1207$02.00

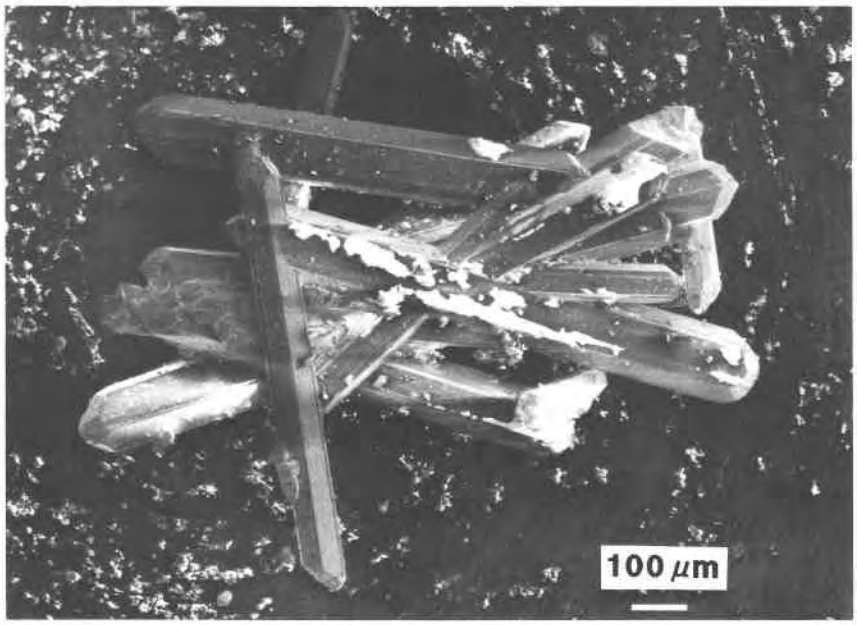

Fig. 1. SEM photograph of a cluster of doubly terminated, pseudohexagonal, natural hectorfloresite crystals.

and found to contain Na, I, and S. This suggested a sodium-iodate-sulfate mineral in the system $NaIO_3$-Na_2SO_4-H_2O, which had been studied by Foote and Vance (1930). We restudied this system to confirm the results of Foote and Vance and found that one of the two double salts forming in the system, $NaIO_3 \cdot 4Na_2SO_4$, gave an X-ray powder-diffraction pattern identical to that of natural hectorfloresite.

Although found at only one locality, the new mineral may be a widespread minor constituent of the Chilean nitrate deposits and could account for a significant amount of the ubiquitous iodine that has supplied most of the world's iodine since the mid-19th century. These deposits remain a major source of iodine today, but since the mid-20th century, Chilean iodine production has been surpassed by Japanese production of iodine from gas-well brines. Other iodate minerals in the Chilean nitrate deposits—lautarite $[Ca(IO_3)_2]$, brüggenite $[Ca(IO_3)_2 \cdot H_2O]$, and dietzeite $[Ca_2(IO_3)_2(CrO_4)]$—are known to occur in local concentrations, particularly in *caliche amarillo* (yellow nitrate ore), but appear to be absent in the typical nitrate ore containing an average of 0.03–0.06 wt% IO_3. We believe it is possible that part of this iodate is contained in finely disseminated hectorfloresite intimately mixed with the other saline minerals of the nitrate ore. Such material would be difficult, if not impossible, to recognize in hand specimens.

Hectorfloresite is named for Ing. Hector Flores W. (1906–1984), a much-loved pioneer geologist of Chile, who made important contributions to the understanding of Chilean mineral deposits while working for both government and industry and who was an inspiring teacher at the University of Chile. The new mineral and the name have been approved by the Commission on New Minerals and Mineral Names, IMA. Three specimens, containing a hundred or more hectorfloresite crystals, all the known natural material, and a vial containing about 7 g of impure synthetic material have been deposited in the mineral collection of the U.S. National Museum, Smithsonian Institution, Washington, D.C.

Physical and optical properties

Natural hectorfloresite crystals are white pseudohexagonal prisms that are generally less than 1 mm long and 0.2 mm in diameter; the largest crystals are 1.5 mm long and 0.5 mm in diameter. They show multiple twinning (Fig. 2) parallel to the axis (*b*) of elongation, which gives rise to the pseudohexagonal form. In polarized light, the most perfect twinned crystals, when oriented perpendicular to the axis of elongation, appear to consist of six wedge-shaped prisms so oriented that opposite wedges show parallel extinction. Other crystals show less symmetrical twinning. Because of the small size of crystals, hardness and cleavage could not be determined with precision. By breaking crystals between glass slides it was possible to estimate the hardness to be about 2. The crystals are brittle and show conchoidal fracture. They apparently lack cleavage, although they tend to break along irregular to undulatory parting planes both perpendicular and parallel to the axis of elongation. The specific gravity of synthetic hectorfloresite, determined from a 0.25-g sample in a 1.1-mL pycnometer (immersion liquid was tetrachloraethylene) at room temperature, is 2.80(3). The density calculated from the X-ray data (see below) is 2.90 g/cm^3.

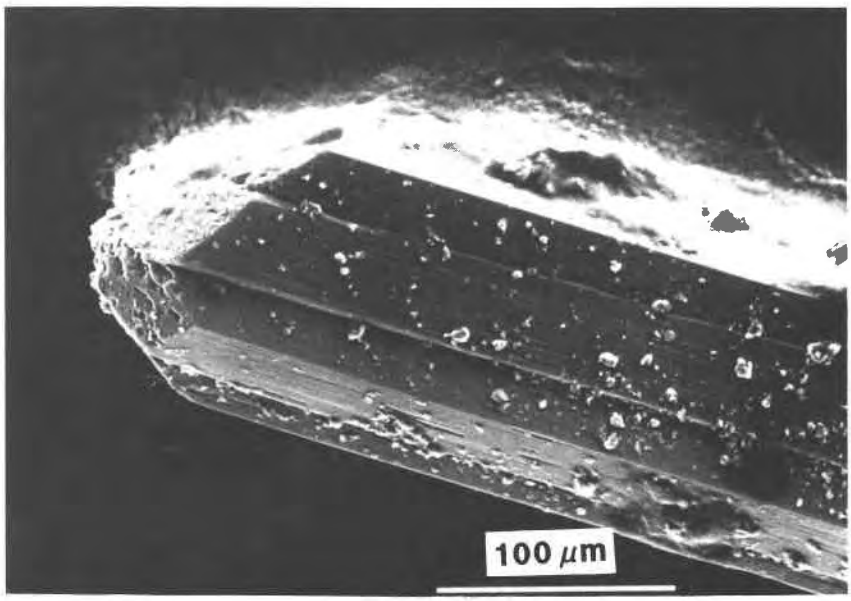

Fig. 2. SEM photograph of a multiply twinned, pseudohexagonal, natural hectorfloresite crystal, showing four prismatic wedge-shaped twins and fluid-inclusion cavities on pyramidal faces.

In transmitted light, hectorfloresite is colorless, but in polarized light, crystals are seen to contain abundant, dark, tubular fluid-inclusion cavities oriented parallel to the axis of elongation. The above-mentioned pattern of parting planes is at least in part controlled by the distribution of these cavities. A few of the cavities contain fluid (under polarized light, both gas and liquid phases can be recognized), but apparently most cavities are now dry. The cavities show as pits on terminal pyramid faces of crystals (Fig. 2).

Natural hectorfloresite is biaxial negative, with $2V_X = 26(2)°$. Indices of refraction, determined for natural crystals in monochromatic Na light at room temperature, with refractive-index liquids measured with a Leitz-Jelly refractometer for each determination, are $\alpha = 1.493(2)$, $\beta = 1.521(2)$, and $\gamma = 1.523(2)$. Dispersion, $r < v$, is barely discernible. Indices of refraction of synthetic hectorfloresite (α and γ measured, β calculated) are the same as those for natural crystals.

Crystallography

The pseudohexagonal crystals of natural hectorfloresite show well-reflecting prism faces and pitted terminal faces set at 30° to the prisms around the prism axis (Figs. 2 and 3). The crystals are composite, showing multiple twinning parallel to the axis (monoclinic b) of elongation. As a consequence, precession X-ray photographs show a definite period of 6.94 Å along the b (pseudohexagonal) axis, but completely twinned nets normal to this axis. Figure 4 shows a typical pseudohexagonal, zero-level precession pattern of a multiply twinned natural crystal. After considerable study of enlarged images of this pattern, a monoclinic lattice was identified that, when twinned six times around the monoclinic b axis, would account for every reflection in the pattern. Upper-level patterns clearly show the presence of a glide plane.

By good fortune, a crystal fragment from a broken hexagonal prism of natural hectorfloresite was proven by precession photography to consist of about 95% untwinned crystal. Patterns of this crystal fully confirmed the monoclinic cell identified in precession patterns of twinned crystals. In addition, this crystal fragment was used to obtain an intensity data set from which the crystal structure of hectorfloresite has been deduced. A predicted powder pattern calculated from this structural data greatly improved the accuracy of indexing of the powder pattern for synthetic material.

Debye-Scherrer X-ray powder-diffraction patterns of

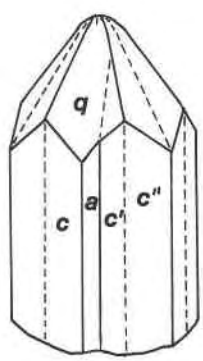

Fig. 3. Perspective sketch of a multiply twinned hectorfloresite crystal, showing prism faces $a(100)$ and $c(001)$ and a pyramid face $q(212)$; the forms c and q are representative of the hexagonal sublattice.

TABLE 1. X-ray powder data for synthetic and natural hectorfloresite, $Na_9(IO_3)(SO_4)_4$

				Synthetic			Natural		Thenardite	
h k l	I_{calc}	d_{calc}	I/I_0*	d_{obs}*	I/I_0†	d_{obs}†	I/I_0‡	d_{obs}‡	I/I_0§	d_{obs}§
0 0 1	9	13.47	3	13.44	3	13.45	3	13.44		
2 0 0	16	8.84	5	8.86	5	8.87	7	8.86		
0 0 2	9	6.74	6	6.72	6	6.74	1	6.70		
2 0 1	5	6.51								
$\bar{2}$ 0 2	7	6.47	2	6.48	5	6.49	1	6.41		
0 1 1	11	6.17	10	6.16	6	6.17	10	6.17		
$\bar{1}$ 1 1	33	6.11								
1 1 1	15	5.57								
$\bar{2}$ 1 1	13	5.46	10	5.46	6	5.46	8	5.45		
0 1 2	5	4.83	2	4.84	1	4.84				
2 1 1	6	4.75	2	4.75						
$\bar{4}$ 0 1	19	4.69	10	4.69	32	4.68	15	4.69	73	4.66
2 0 2	15	4.68								
$\bar{2}$ 0 3	17	4.66								
$\bar{3}$ 1 1	13	4.63								
1 1 2	10	4.41	3	4.44	3	4.44	3	4.42		
3 1 1	7	3.985					2	4.30		
$\bar{1}$ 1 3	7	3.909								
$\bar{4}$ 1 1	87	3.887	100	3.891	60	3.880	100	3.880	18	3.84
2 1 2	84	3.882								
$\bar{2}$ 1 3	100	3.869	30	3.869						
$\bar{3}$ 1 3	10	3.663								
1 1 3	2	3.499	2	3.518						
0 2 0	28	3.468	7	3.469	2	3.470	6	3.470		
1 2 0	10	3.404								
3 1 2	7	3.378								
$\bar{4}$ 1 3	7	3.360	4	3.363	4	3.360	3	3.360		
0 2 1	4	3.358								
2 2 0	15	3.230	15	3.232	2	3.232	3	3.240		
5 1 0	9	3.162	3	3.170	4	3.176			51	3.178
$\bar{1}$ 1 4	10	3.142								
$\bar{1}$ 2 2	8	3.117								
$\bar{6}$ 0 1	6	3.110			4	3.109				
0 2 2	15	3.083	6	3.081	5	3.080	8	3.081	47	3.075
$\bar{2}$ 2 2	15	3.056	10	3.058	2	3.058				
0 1 4	6	3.029	2	3.030	2	3.032	4	3.038		
$\bar{5}$ 1 3	7	3.029								
$\bar{3}$ 2 2	9	2.918	2	2.934	2	2.942	2	2.928		
$\bar{4}$ 2 1	36	2.789	7	2.813						
2 2 2	45	2.787	80	2.788	20	2.785	30	2.788	100	2.783
$\bar{2}$ 2 3	24	2.782								
0 2 3	10	2.745	2	2.745						
$\bar{4}$ 2 2	4	2.729	3	2.731						
6 0 1	89	2.713	30	2.711						
$\bar{6}$ 0 4	84	2.703	50	2.700	100	2.700	80	2.700		
0 0 5	76	2.699								
1 2 3	4	2.635	3	2.647	6	2.645	2	2.645	48	2.646
2 2 3	14	2.487	6	2.487	2	2.485	2	2.486		
					2	2.422	2	2.418		
2 0 5	9	2.373	5	2.373	10	2.370	6	2.372		
4 2 2	8	2.373								
$\bar{4}$ 2 4	12	2.366	5	2.366						
$\bar{8}$ 0 2	7	2.347	7	2.344	12	2.344	6	2.342	21	2.329
4 0 4	11	2.342								
$\bar{6}$ 2 1	7	2.315	6	2.314	7	2.310	2	2.310		
8 0 1	11	2.314								
0 3 1	6	2.279	8	2.279						
$\bar{6}$ 2 3	2	2.247	1	2.247						
0 0 6	2	2.245								
$\bar{3}$ 1 6	3	2.242								
$\bar{2}$ 1 6	2	2.240								
$\bar{2}$ 3 1	2	2.237	3	2.237	3	2.240	2	2.236		
2 3 0	2	2.237								
$\bar{2}$ 2 5	9	2.200	2	2.202	4	2.205	1	2.200		
$\bar{6}$ 0 6	14	2.157	6	2.156	8	2.155	5	2.152		

TABLE 1.—*Continued*

			Synthetic				Natural		Thenardite	
h k l	I_{calc}	d_{calc}	I/I_0*	d_{obs}*	I/I_0†	d_{obs}†	I/I_0‡	d_{obs}‡	I/I_0§	d_{obs}§
8 1 0	3	2.114	2	2.115						
$\bar{4}$ 3 1	5	2.074								
2 3 2	7	2.073	8	2.072	3	2.072	5	2.079		
0 3 3	12	2.055	6	2.055	2	2.055	5	2.050		
4 3 0	9	2.051	2	2.047						
$\bar{4}$ 3 3	10	1.9806	7	1.9810	1	1.9800	3	1.9800		
$\bar{8}$ 2 2	18	1.9436	15	1.9420	10	1.9430	20	1.9420		
4 2 4	19	1.9411								
$\bar{4}$ 2 6	17	1.9343	2	1.9333						
$\bar{8}$ 2 1	6	1.9250								
$\bar{8}$ 2 3	5	1.9223			2	1.9229				
4 3 2	8	1.8846	4	1.8842			1	1.8846		
6 1 4	2	1.8636	6	1.8647	3	1.8630	2	1.8647	31	1.864
$\bar{6}$ 3 3	8	1.8195	6	1.8193			2	1.8193		
2 3 4	4	1.7971	4	1.7972			1	1.7972		
$\bar{2}$ 3 5	4	1.7947								
0 4 0	15	1.7339	10	1.7399			2	1.7339		
$\bar{5}$ 1 8	3	1.7040			3	1.7120	2	1.7143		
2 4 0	4	1.7018	4	1.7016						
6 3 2	9	1.6765	5	1.6804	8	1.6780	10	1.6800		
$\bar{2}$ 3 6	6	1.6537	3	1.6534						
$\bar{10}$ 2 3	4	1.6474								
$\bar{8}$ 3 2	5	1.6469	3	1.6462	2	1.6434	3	1.6461		
4 3 4	3	1.6454								
$\bar{1}$ 3 6	6	1.6386								
$\bar{10}$ 2 1	3	1.6253	4	1.6254			1	1.6274		
4 4 0	2	1.6151								
$\bar{4}$ 4 2	2	1.6143	4	1.6147						
0 3 6	4	1.6016								
$\bar{8}$ 3 4	6	1.5983	2	1.5981						
10 2 0	5	1.5808	2	1.5811			3	1.5814		
8 2 3	3	1.5798	2	1.5780						
$\bar{8}$ 2 7	5	1.5726	5	1.5728	2	1.5730	5	1.5730		
2 2 8	4	1.5709								
12 0 3	12	1.5645	2	1.5628						
6 0 6	12	1.5616	10	1.5602	7	1.5607	10	1.5607		
2 4 3	6	1.5595								
$\bar{6}$ 0 9	9	1.5537	2	1.5535			10	1.5533		

Note: All reflections for which $d > 1.5500$ and $I \geq 2$ (I calculated from crystal structure) are included.

* Guinier-Hägg pattern for synthetic hectorfloresite. The pattern was made with Cu$K\alpha_1$ radiation ($\lambda = 1.540562$ Å) and an Si internal standard (NBS SRM 640), and relative intensities were estimated visually.

† Diffractometer pattern of synthetic hectorfloresite. The pattern was made with Cu$K\alpha_1$ radiation by a Diano automatic recording X-ray diffraction unit. Relative intensities and d values are averages of the most consistent values from numerical printouts of several patterns of the samples shown in Table 2.

‡ Debye-Scherrer film of natural hectorfloresite. The pattern was made with Cu$K\alpha_1$ using a ball mount without an internal standard, and the relative intensities were estimated visually.

§ From Swanson and Fuyat (1953) for type V Na_2SO_4; only lines having relative intensities greater than 15 are included.

synthetic hectorfloresite correspond precisely (within limits of measurement) to patterns of natural material. Guinier-Hägg films of synthetic material (Table 1) show essentially the same reflections as the Debye-Scherrer films of both natural and synthetic material, but because of better resolution also show additional lines. The diffractometer patterns (Table 1) are in close agreement with the Debye-Scherrer patterns except for a few reflections that occur in one type of pattern but not in the other and minor differences in intensities of the strongest reflections, $d = 3.880$ Å, 2.700 Å, and 4.69 Å. These discrepancies in intensities may be due to a variety of factors, including (1) preferred orientation, which would have the greatest effect on diffractometer determinations; (2) imprecise visual estimates of relative intensities; and (3) inherent differences in the resolution afforded by each method.

The unit cell identified in precession patterns of natural hectorfloresite was used to index the powder pattern of the synthetic material, which in turn was used to refine the unit-cell parameters by least-squares analysis. The best unit-cell refinement is based on least-squares analysis of 34 unambiguously indexed lines from a Guinier-Hägg pattern, as indicated by the calculated pattern. The refined monoclinic unit cell has the following parameters: $a = 18.775(4)$ Å, $b = 6.9356(7)$ Å, $c = 14.239(2)$ Å, and

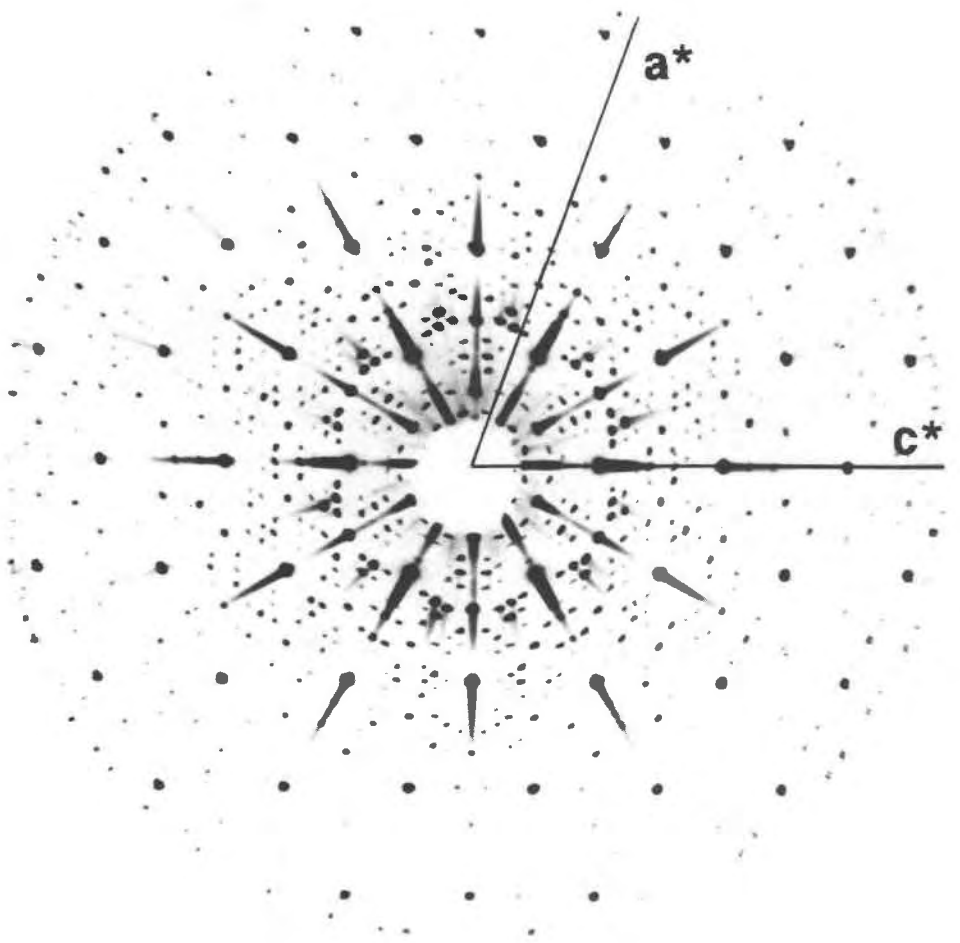

Fig. 4. Zero-level precession pattern showing the multiply twinned, pseudohexagonal net of hectorfloresite. The hexagonal distribution of the strongest reflections is due to the type I Na_2SO_4 hexagonal subcell. The reciprocal monoclinic axes are labeled a^* and c^*.

$\beta = 108.91(2)°$. The cell contains 4 units of $Na_9(IO_3)(SO_4)_4$, and the volume $V = 1754.0(4)$ Å^3. The space group is $P2_1/a$.

The synthetic hectorfloresite contains about 18% type V Na_2SO_4 (thenardite), which apparently did not have any significant effect on the d values and relative intensities of hectorfloresite. As can be seen in Table 1, all the strong thenardite lines, except $d = 3.181$ Å, correspond to reflections of both natural and synthetic hectorfloresite. The 3.181-Å reflection does not appear in the Debye-Scherrer patterns for natural material, but a 3.162-Å reflection that appears in precession patterns of natural crystals of hectorfloresite may correspond to the 3.170 Å (3.176 Å) lines in the Guinier-Hägg and diffractometer patterns. Comparison is made with thenardite because this is the stable form that crystallizes from water at 50 °C, the temperature at which the synthetic hectorfloresite was prepared. According to Foote and Vance (1930), $Na_9(IO_3)(SO_4)_4$ is stable only above 30 °C.

The crystal structure of hectorfloresite is based on that of the type I Na_2SO_4 phase, which is stable above 271 °C, is hexagonal, with $a = 5.39$ Å and $c = 7.02$ Å (extrapolated to 25 °C), and has a cell content of 2 formula units (Fischmeister, 1962). The zero-level precession pattern (Fig. 4) shows the sixfold symmetry of this cell. The monoclinic hectorfloresite unit cell has 10 times the volume of the type I Na_2SO_4 cell and has an ordered hexagonal substructure in which every fifth sulfate group is replaced by an iodate group. Evidently, many of the strongest lines that are not resolved in the powder pattern (Table 1) belong to the strong hexagonal subcell. Details of the structure will be published elsewhere.

The monoclinic symmetry of the unit cell of hectorfloresite can be reconciled with the external form of natural crystals. The twin and composition planes are all parallel to the b axis and strongly reflect the hexagonal subcell symmetry. The twin planes are $c(001)$, (601), and $(\bar{6}04)$, and the corresponding composition planes are close to

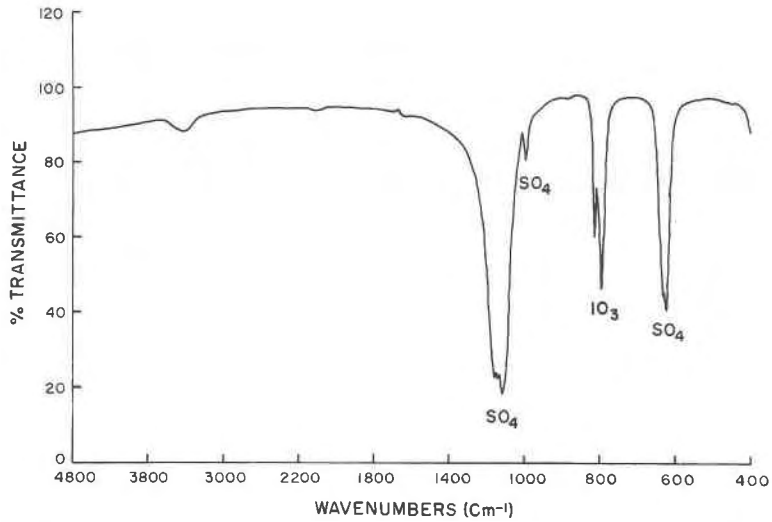

Fig. 5. Infrared spectrum of synthetic hectorfloresite, showing absorption peaks for SO_4 and IO_3.

(202), ($\bar{4}01$), and ($\bar{2}03$). These planes are all 30 ± 0.5° away from adjacent planes. Commonly, the twin components are not equally developed, and re-entrants may appear on the prism surface because of the presence of the *a*(100) face of a neighboring twin at a dihedral angle of 11°. Such re-entrants are shown in Figures 2 and 3. The predominant terminal face is *q*(212) [or ($\bar{4}11$) or ($\bar{2}13$)], which is inclined to the *b* axis at 56.0°. The forms *c* and *q* are representative of the hexagonal sublattice. Other forms, such as {$\bar{2}11$}, also have been observed. Terminal faces are pitted and crystal tips are rough and rounded (Figs. 2 and 3) because of the abundant fluid-inclusion cavities.

Chemical composition

The chemical composition of hectorfloresite (Table 2) was determined by wet-chemical analyses of synthetic material prepared by crystallization in the system $NaIO_3$-Na_2SO_4-H_2O at 50 °C. The two double salts shown in the table were obtained as residues from various mixtures of the components, as reported by Foote and Vance (1930). For example, the solution from which sample EFL-26 (Table 2) was obtained was prepared by first dissolving 3.0 g of $NaIO_3$ in 76.4 g of distilled water, and then adding 40.6 g of Na_2SO_4, all at a constant temperature of 50 °C. Samples EFL-22 and EFL-27 (Table 2) were obtained from solutions containing slightly different amounts of the components, but from which Foote and Vance also obtained residues in which $Na_9(IO_3)(SO_4)_4$ was the only double salt. In contrast, EFL-23 and EFL-24 were made from solutions containing significantly more iodate and less sulfate. EFL-24, for example, was made from a solution consisting of 82.1 g H_2O, 6.1 g $NaIO_3$, and 31.9 g Na_2SO_4. In the runs from which the double salts were obtained, both the iodate and sulfate were completely dissolved to make a clear solution, which after about 2 min suddenly formed a thick white precipitate, consisting chiefly or wholly of the double salts. In order to assure equilibrium, these mixtures were held at 50 °C, in closed flasks in an oven, for two weeks, with periodic shaking. The liquid phase was then decanted, and the wet residue, consisting of a felted mass of tiny (<0.5 mm long and <0.1 mm in diameter) prismatic crystals, was recovered on filter paper. The residue was dried at 50 °C, and both the dried residue and the liquid phase were analyzed. Table 2 shows both the original analyses of the residues and the recalculated analyses from which the contaminants of the liquid phase trapped in the wet residue were removed. The contaminating phases in the three samples are (in wt%) 17.5–18.5% Na_2SO_4 and 0.1–0.6% $NaIO_3$. As can be seen in Table 2, the recalculated analyses for synthetic hectorfloresite, which was identified by X-ray diffraction, correspond to the compound $Na_9(IO_3)(SO_4)_4$. This compound and the second double salt, Na_7-

Table 2. Chemical analyses (wt%) of synthetic and natural hectorfloresite, and a second double salt, $Na_7(IO_3)(SO_4)_3$.

	Chemical analyses*			Recalculated analyses**		
	Na_2O	I_2O_5	SO_3	Na_2O	I_2O_5	SO_3
$Na_9(IO_3)(SO_4)_4$						
EFL-22 (synthetic)	37.0	18.58	44.3	35.3	22.1	42.5
EFL-26 (synthetic)	36.0	17.79	44.5	35.1	22.1	42.8
EFL-27 (synthetic)	36.2	17.69	44.8	35.3	21.8	42.9
Theoretical				36.4	21.8	41.8
Natural†				34.5	23.2	42.3
$Na_7(IO_3)(SO_4)_3$						
EFL-23	34.7	21.76	42.0	33.3	26.8	39.9
EFL-24	34.6	23.18	41.0	33.9	26.6	39.5
Theoretical				34.8	26.7	38.5

* Samples were moist residues dried at 50 °C.

** Recalculated to eliminate $NaIO_3$ and Na_2SO_4 contaminants in solutions trapped in moist residues (see text).

† Averages of eight microprobe determinations showing following ranges (wt%): 33.2–37.0 Na_2O, 22.0–24.5 I_2O_5, and 40.6–43.4 SO_3.

$(IO_3)(SO_4)_3$, shown in Table 2, correspond to the two compounds found by Foote and Vance (1930).

Both natural and synthetic hectorfloresite were analyzed by electron microprobe (Table 2) using Bence and Albee (1968) correction procedures. These analyses were difficult because of the sensitivity of the material to electron-beam damage and because of poor polishing characteristics. The Na measurements were found to change noticeably with time in single determinations, probably because of thermal and charging effects caused by the electron beam. Spurious results for Na also caused inaccuracies in determining the concentrations of S and I.

After repeated attempts to improve the analytical measurements, it was found that the most consistent analyses were obtained with a 10-kV accelerating voltage, a 0.04-μA beam current, a 10-s counting time, and a rapidly moving beam spot. Albite (Na), synthetic $Ca(IO_3)_2$ (I), and anhydrite (S) were used as standards. Microprobe determinations for Na, I, and S in hectorfloresite also were checked against microprobe analyses of thenardite and synthetic $NaIO_3$. The averages of eight microprobe determinations (Table 2) indicate that the natural material has a composition corresponding to $Na_9(IO_3)(SO_4)_4$. Preliminary microprobe analyses of synthetic material indicate a similar composition.

One of the natural crystals that was analyzed by microprobe was found to have an intergrown phase having an average composition of 32.4 wt% Na_2O, 26.3 wt% I_2O_5, and 38.4 wt% SO_3, which may correspond to $Na_7(IO_3)(SO_4)_3$, the second phase in the system. The amount of this material is evidently small and is believed to have no affect on the bulk composition determined for synthetic hectorfloresite.

The compatibility index $[1 - (K_P/K_C)]$, which is the Gladstone-Dale relationship between chemical composition, refractive indices, and density, was calculated for hectorfloresite. Using the composition indicated by the formula, the measured refractive indices, and the measured density of 2.80 g/cm^3, the index was found to be 0.015, which is superior (Mandarino, 1979). If the calculated density of 2.90 g/cm^3 is substituted for the measured density, the index is 0.047, which is good.

Infrared characteristics

The infrared spectrum (Fig. 5) shows characteristic absorption peaks for IO_3 and SO_4. The peaks for IO_3 are at $\nu_1 = 790$ cm^{-1} and $\nu_3 = 810$ cm^{-1}, both of which are due to stretching vibrations (Nakamoto, 1963). The peaks for SO_4 are at $\nu_1 = 995$ cm^{-1} and $\nu_3 = 1120$–1140 cm^{-1}, both of which also are due to stretching vibrations, and $\nu_4 = 620$ cm^{-1}, which is due to planar bending (Ross, 1974).

Acknowledgments

This study is part of a broad investigation of the Chilean nitrate deposits being carried out jointly by the Servicio National de Geología y Minería of Chile and the U.S. Geological Survey. The infrared spectrum was made by John W. Salisbury and the S analyses of synthetic hectorfloresite by Norma Rait, both of the U.S. Geological Survey, Reston, Virginia.

References cited

Bence, A.E., and Albee, A.L. (1968) Empirical correction factors for the electron microanalysis of silicates and oxides. Journal of Geology, 76, 382–403.

Fischmeister, H.F. (1962) Röntgenkristallographische Ausdehnungsmessungen an einigen Alkalisufaten. Ein Beitrag zur Kenntnis der Anionenfehlordnung in Na_2SO_4 I-typ. Monatshefte der Chemie, 93, 420–434.

Fleischer, M. (1987) Glossary of mineral species, 5th edition, 227 p. Mineralogical Record, Tucson, Arizona.

Foote, H.W., and Vance, J.E. (1930) The ternary system: Sodium iodate–sodium sulphate–water. American Journal of Science, 5th series, XIX, 203–213.

Mandarino, J.A. (1979) The Gladstone-Dale relationship. Part III: Some general applications. Canadian Mineralogist, 17, 71–76.

Nakamoto, K. (1963) Infrared spectra of inorganic and coordination compounds, 328 p. Wiley, New York.

Ross, S.D. (1974) Sulfates and other oxy-anions of Group VI. In V.C. Farmer, Ed., The infrared spectra of minerals. Mineralogical Society Monograph 4, 423–444.

Swanson, H.E., and Fuyat, R.K. (1953) Standard X-ray diffraction patterns. National Bureau of Standards Circular 539, 59–60.

Manuscript received January 18, 1989
Manuscript accepted June 3, 1989